Spectrochimica Acta Part A: Molecular and Biomolecular Spectroscopy 304 (2024) 123305

Contents lists available at ScienceDirect

Spectrochimica Acta Part A: Molecular and Biomolecular Spectroscopy

journal homepage: www.journals.elsevier.com/spectrochimica-acta-part-a-molecular-and-biomolecular-spectroscopy

Expression data of FOS and JUN genes and FTIR spectra provide diagnosis of thyroid carcinoma

João Paulo da Silva Queiroz [a], Breno Pupin [a], Tanmoy Tapobrata Bhattacharjee [b], Miyuki Uno [c], Roger Chammas [c], Marco Aurélio Vamondes Kulcsar [d], Renata de Azevedo Canevari [a,*]

[a] Laboratório de Biologia Molecular do Câncer, Universidade do Vale do Paraíba, UNIVAP, Instituto de Pesquisa e Desenvolvimento, Avenida Shishima Hifumi 2911, Urbanova, São José dos Campos, 12244-000 São Paulo, SP, Brazil
[b] Sir John Walsh Research Institute, University of Otago, 310 Great King St, North Dunedin, Dunedin 9016, New Zealand
[c] Centro de Investigação Translacional em Oncologia, Departamento de Radiologia e Oncologia, Instituto do Cancer do Estado de São Paulo (ICESP), Faculdade de Medicina da Universidade de São Paulo (FMUSP), Avenida Dr. Arnaldo 251, Cerqueira César, São Paulo 01246-000, São Paulo, Brazil
[d] Serviço de Cirurgia de cabeça e Pescoço, Instituto do Câncer do Estado de São Paulo - ICESP, Av. Doutor Arnaldo, 251, Cerqueira César, CEP 01246-000 São Paulo, SP, Brazil

HIGHLIGHTS

- FOS and JUN genes are potential diagnostic marker in thyroid carcinomas.
- ATR-FTIR could identify thyroid carcinoma with high efficiency.
- ATR-FTIR and qRT-PCR analysis are highly sensitive to distinguish thyroid lesions.

GRAPHICAL ABSTRACT

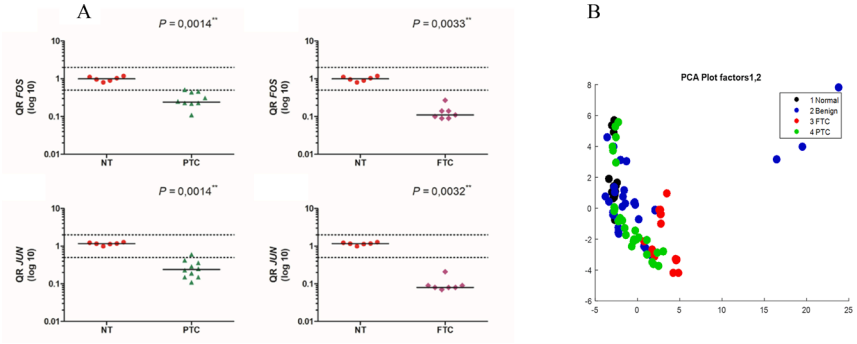

ARTICLE INFO

Keywords:
Thyroid cancer
Diagnosis
FTIR
Gene expression
FOS
JUN

ABSTRACT

We explore the feasibility of using FOS and JUN gene expression and ATR-FTIR for diagnosis of thyroid cancer. For the study, 38 samples (6 non-neoplastic (NN), 10 papillary thyroid carcinoma (PTC), 7 follicular thyroid carcinoma (FTC), and 15 benign tumors (BT) were subjected to RNA extraction followed by quantitative real time PCR (qRT-PCR) and 30 samples (5 NN, 9 PTC, 5 FTC, and 11 BT) were used for Attenuated Total Reflectance – Fourier Transform Infrared (ATR-FTIR) followed by multivariate analysis. Of the above, 20 samples were used for both gene expression and ATR-FTIR studies. We found FOS and JUN expression in malignant tumor samples to be significantly lower than NN and benign. ATR-FIR after multivariate analysis could identify the difficult to diagnose FTC with 93 % efficiency. Overall, results suggest the diagnostic potential of molecular biology techniques combined with ATR-FTIR spectroscopy in differentiated thyroid carcinomas (PTC and FTC) and BT.

* Corresponding author at: Universidade do Vale do Paraíba, Instituto de Pesquisa e Desenvolvimento, Laboratório de Biologia Molecular do Câncer, Avenida Shishima Hifumi 2911 - Urbanova, São José dos Campos 12244-000, Brazil.
E-mail address: rcanevari@univap.br (R. de Azevedo Canevari).

https://doi.org/10.1016/j.saa.2023.123305
Received 8 May 2023; Received in revised form 11 August 2023; Accepted 26 August 2023
Available online 28 August 2023

1. Introduction

Thyroid cancer is the most common malignancy affecting the endocrine system. Its incidence has increased over the last few years due advancements in diagnostic techniques and resultant early identification of nodules [1–3]. GLOBOCAN estimates showed that in 2020, thyroid cancer represented 3 % of cancer cases diagnosed worldwide in both genders, establishing itself as the ninth most frequent, however, affecting three times more women than men [4]. In Brazil, this neoplasm is six times more prevalent among women compared to men. The National Cancer Institute estimated 11,950 new cases among women as opposed to 1,830 among men in 2020 [5].

Papillary thyroid carcinoma (PTC) and follicular thyroid carcinoma (FTC) are well differentiated tumors and more frequent, representing 50 to 80 % and 15 to 20 % of diagnosed cases, respectively [5]. PTC tumors progress slowly and gradually, and may develop capsular invasion and, consequently, infiltration of adjacent tissues [6], favoring metastasis in lymph nodes adjacent to the gland [7]. In contrast, their prognosis is better compared to FTC, since the latter are difficult to diagnose and are identified only after the staging of capsular or vascular invasion [8], and can rapidly metastasize to lung and bone [9].

Currently, ultrasound (US) imaging is used most frequently method to check nodes that are not palpable at the time of clinical diagnosis [10], and the fine-needle aspiration biopsies (FNAB) [11] is used to collect thyroid tissue samples for cytological analysis. However, the rate of lesions with cytological indeterminate results in this analysis and the difficulty of diagnosis in small tumors are still factors that limit the clinical conduct [12–13]. Therefore, the use of new techniques associated with cytological analysis can provide a more accurate diagnosis.

Molecular biology techniques, in particular gene expression analyzes [14–16], is an important tool in the identification of molecular markers that can categorize the different histological types of thyroid carcinomas. These techniques have many advantages compared to cytology and histopathological analysis, such as a higher sensitivity and specificity in differentiating benign, malignant and normal tissue [17–18]. In this sense, it can assist in the diagnostic support and in the more accurate determination of patient outcomes [19–22].

FOS and JUN genes are proto-oncogenes that encode the AP-1 complex transcription factor [23]. Together, the proteins make up the protein complex of activator protein-1 (AP-1), a major component in the Mitogen Activated Protein Kinase (MAPK/Kinase) signaling pathway. The pathway is involved in the development of thyroid carcinomas [24–25] by activating cellular processes such as proliferation, differentiation and apoptosis [26–27]. The alteration in the expression of one or more genes involved in the activation of the MAPK/Kinase pathway may lead to the development of tumors and, consequently, the identification of these alterations, such as FOS and JUN genes, can provide a more accurate and sensitive diagnosis [28].

While accurate and sensitive, gene expression based diagnostic techniques can be time-consuming and require high investments in the acquisition of reagents, equipment, and specialized labor, demonstrating the need to develop techniques more accessible that present the same precision. Vibrational spectroscopic techniques such as Fourier transform infrared spectroscopy (FTIR), can aid rapid, objective, and easy-to-use diagnosis of the tumors [29–36]. Vibrational changes observed by FTIR spectroscopy in the intensity of the nucleic acid bands DNA and RNA, may be correlated with normal cellular processes and genotypes of pathological character, manifest as mutations genome and changes in gene expression in the tumor cells [37–38].

Therefore, in this study, we conducted FOS and JUN gene expression analysis using quantitative real time PCR (qRT-PCR) and ATR-FTIR spectroscopy to discriminate differentiated thyroid carcinomas (PTC and FTC) and BT. The aim is to find molecular and spectral markers to diagnose these tumors, and improve clinical outcomes for patients.

2. Materials and methods

2.1. Ethical aspects

This study was approved by the Research Ethics Committee of the University of Vale do Paraíba under number 3,620,075/CEP/2019. The thyroid tissue samples were obtained from Academic Biobank for Research on Cancer at the University of Sao Paulo (USP), Instituto do Cancer do Estado de São Paulo (ICESP), São Paulo, Brazil. The Biobank was approved by local and National Ethics Committees (Protocols 031/2012 and 023/2014, respectively).

2.2. Samples

Fresh frozen tissues of primary tumors (tumoral and non-neoplastic) from surgery (total thyroidectomy) were collected in liquid nitrogen from 48 patients with thyroid cancer, and, later, these samples were stored in the −80 °C Freezer. Tissue samples were analyzed and underwent histopathological diagnosis with reports signed by the Department of Pathology, Instituto do Cancer do Estado de São Paulo (ICESP), following the diagnostic protocol of the Brazilian Society of Pathology (BSP) for thyroid cancer, and all samples were macrodissected with a scalped to ensure that only sections composed at least 80 % tumor cells be included in the study.

For gene expression studies, 38 samples were used, including 15 samples of benign thyroid (BT) lesions (6 samples of adenomatous goiter, 5 samples of follicular adenoma and 4 samples of follicular hyperplasia), 10 samples of PTC, 7 samples of FTC and 6 samples of non-neoplastic (NN) tissue.

For the ATR-FTIR spectroscopy technique, 30 samples were used − 11 BT lesions (5 samples of adenomatous goiter, 4 follicular adenoma and 2 follicular hyperplasia), 9 samples of PTC, 5 samples of FTC and 5 samples of NN tissues. Of the above, 20 samples were used for both gene expression and ATR-FTIR studies. The number of samples between the groups and techniques were in different amounts due to the limited size of the sectioned tumors, since in some cases the samples were enough to perform only one technique.

2.3. Samples design

For gene expression analysis by qRT-PCR, the samples were divided into five groups: group 1: NN tissues of thyroid, group 2: benign tissues (BT) (adenomatous goiter, follicular adenoma and follicular hyperplasia), group 3: malignant tissue (PTC and FTC), group 4: PTC, and group 5: FTC. Theses samples were compared performing the analysis 1 (group 3 vs group 1), analysis 2 (group 4 vs group 1), analysis 3 (group 5 vs group 1), analysis 4 (group 3 vs group 2), analysis 5 (group 4 vs group 2), analysis 6 (group 5 vs group 2) and analysis 7 (group 5 vs group 4). For FTIR analysis, the samples were divided into four groups: samples of NN tissue (group 1), BT samples (group 2), PTC samples (group 3) and FTC samples (group 4) and compared to each other.

2.4. Gene expression analysis

FOS and JUN genes were selected based on results of our previous of PCR array studies conducted by our research group, in which differential expression in 34 genes from a total of 84 belonging to the MAPK/ERK pathway (MAP Kinase Signaling pathway platform, PAHs-061ZA-24, SA Biosciences, Qiagen) were detected in the comparison between these sample groups [39]. The MRLP19 gene was defined as endogenous control based on quantification data in samples of the target histological types.

RNA extraction of the samples was performed using the protocols of Rneasy Mini Kit (Qiagen) and Trizol® Reagent (Life Technologies), according to tissue availability. After extraction, the RNA was purified using the RNeasy® MinElute™ Cleanup Kit (Qiagen) protocol and

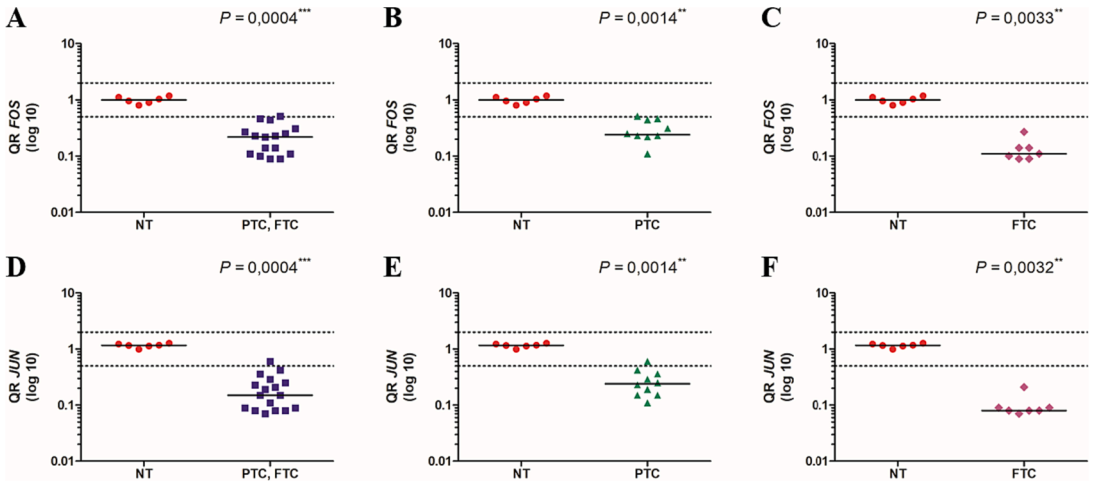

Fig. 1. Relative gene expression by qRT-PCR of the FOS (A, B, C) and JUN (D, E, F) transcripts in thyroid lesions. A e D: comparison between malign tumors (PTC, FTC) with non-neoplastic tissues (NNT) (Analysis 1); B e E: PTC compared with NNT (Analysis 2) and C e F: FTC compared with NNT (Analysis 3).

digested using the DNase I Amplification Grade kit (1U/μL). The qualitative and quantitative characteristics of the RNA was evaluated by ultraviolet absorption spectroscopy on the NanoDrop equipment (ND 1000 Spectrophotometer v.3.0.1, Labtrade). For the evaluation of the RNA integrity, approximately 500 ng was applied on 2 % agarose gel in Tris-Borate-EDTA 1X (TBE) stained with Ethidium Bromide (3 μg/ml).

cDNA synthesis was performed by the Superscript™ IV pre-amplification system that included SuperScript® IV/RNaseOUT™ Enzyme Mix, 2X First-Strand Reaction Mix, and Ring Buffer (Invitrogen, Life Technologies, Carlsbad, CA). RT-qPCR reactions for target and endogenous genes was used Platinum®SYBR® Green RT-qPCR SuperMix-UDG (Applied Biosystems, Life Technologies, Foster City, CA, USA) in a total volume of 10 μl carried out in duplicate on an ABI Prism 7500 Sequence Detection System (Life Technologies, Foster City, CA, USA). Primers were designed using Primer Express software (version 3.0) (PE Applied Biosystems, Foster City, CA, USA). The final concentration of primers used was the 10 μM for qRT-PCR reaction. The data obtained were translated by Sequence Detection System software, version 2.1, PE Applied Biosystems) and plotted on a graph (fluorescence intensity versus the number of cycles). Standard curves of the targets and endogenous gene showed similar amplification efficiencies (>90 %). The analysis of the standard curve was performed by the slope values, calculated by the formula: $E = 10^{-1/slope-1}$, which the slope values should be close to the value of −3.3. The dissociation curve was obtained for each gene to evaluate the specificity of the initiators used.

The results were analyzed using the Delta-Delta Ct (ΔΔCt) method. For each sample, the ΔCt value = mean value Ct target gene-mean value Ct endogenous gene). To determine ΔΔCt, the ΔCt value of each sample was subtracted from the average ΔCt value of NN samples, and this value was added to formula 2-ΔΔCt and the fold change or relative quantification (QR) values obtained [40]. QR values refers to the amount of transcript for each sample (N times > or < than NN) determined by comparison with samples of NN thyroid tissue.

The decrease in gene expression in the sample was considered when the QR values obtained were less than 0.5 (QR ≤ 0.5), and the increased expression when the QR values were>2.0 (QR > 2.0). Statistical analyzes were performed using the GraphPad InStat version 5.00 software (GraphPad Software, San Diego, CA, USA, https://www.graphpad.com) and non-parametric Mann Whitney test to determine whether the QR was significantly different among the groups of tissues analyzed. The results were considered statistically significant with $p \leq 0.05$.

2.5. Spectroscopy analysis

Samples stored in a freezer at −80 °C were cut and thawed at room temperature, not receiving any preparation for the technique. The sectioned tissue samples were kept in a room with low humidity for one hundred minutes (1 h and 40 min) with the intention of removing excess water present in the sample after the sectioning process. Spotlight 400 FT-IR Imaging System spectrometer (Perkin Elmer, USA) equipped with an ATR unit (diamond surface) was used. The specimens were positioned onto the face of the diamond crystal of the ATR unit and the tip of the micrometre clamp was compressed onto the surface to allow the adequate contact to get a characteristic spectrum. A background of 64 scans was performed prior each analysis. Then, three absorbance spectra were acquired by scanning the specimens 32 times over a 1000–4000 cm^{-1} range at a resolution of 8 cm^{-1} per sample.

For mean spectrum calculation, the spectra from each group were baseline corrected by subtracting a polynomial of order 8, vector normalized and smoothed using OPUS 8. For the evaluation of the average spectra when the variations of intensity and displacement with respect to the appearance of the peaks between spectra, the Origin software (Origin 7.5 SR6, Origin Lab Corp, USA) was used.

For multivariate statistical analysis, all spectra were first derivatized to correct baseline effects, 600–1800 cm^{-1} spectral range was selected, and area normalized. Principal Component Analysis (PCA) was performed on these spectra. The first 10 Principal Components (PCs) were used for Linear Discriminant Analysis (LDA) and was then cross validated using leave one out cross validation (LOOCV). All these operations were carried out using Minitab 16.

Principal Component Analysis is an unsupervised analysis that identifies spectral patterns that differs between groups. It then orders these differences in order of importance, the spectral patterns most distinct get top ranks while the rest get ranks progressively below the first. These ranked spectral pattens are called Principal Components (PCs). Each spectrum used in the analysis is then given scores based on the PCs. These scores are then charted on a scatter plot, called the PCA scatter plot. The plot exhibits spectral differences that exist between the groups being analyzed. If there are differences, the groups will show separate clusters. If not, they will overlap.

Linear Discriminant Analysis (LDA) is a supervised analysis where group information of the spectra is used as input along with the spectra themselves. LDA orients the data in n-dimensional space to maximize inter-group difference and minimize intra-group difference. Since the aim of LDA is maximal separation between groups, there is always the possibility of over-fitting and getting wrong results. To verify that the model is not over-fitted, cross-validation techniques are used. Leave one spectrum out cross validation (LOOCV) is one such technique, where LDA model is built after leaving one spectrum out and the left-out spectrum is predicted using the model built. This is repeated till every

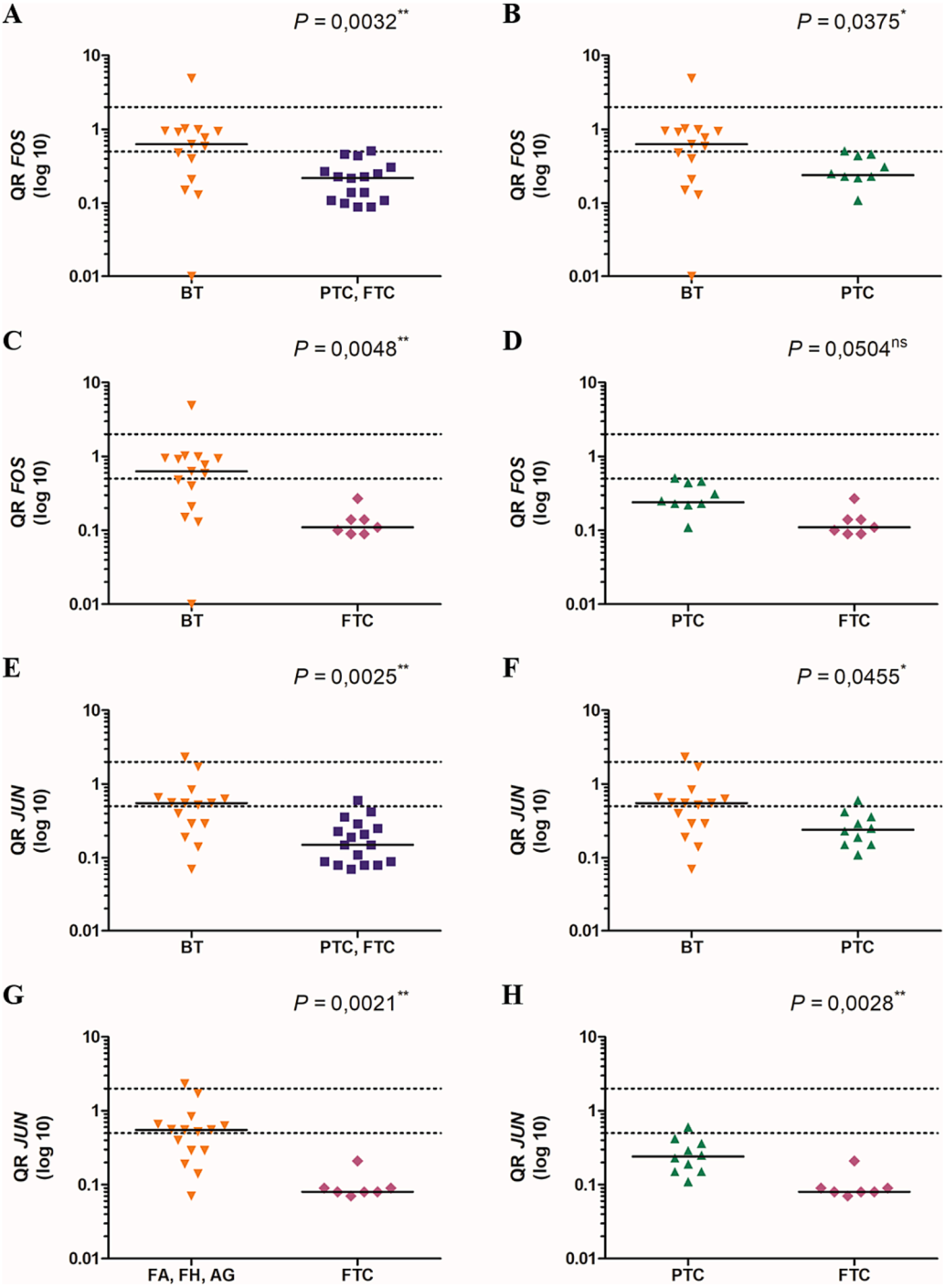

Fig. 2. Relative gene expression by qRT-PCR of the FOS (A, B, C, D) and JUN (E, F, G, H) transcripts in thyroid lesions. A e E: comparison between malign tumors (MT: PTC, FTC) with benign tumors (BT) (Analysis 4); B e F: PTC compared with BT (Analysis 5); C e G: FTC compared with BT (Analysis 6) and D and H: FTC compared with PTC (Analysis 7).

spectrum has been left out once. The prediction for each spectrum is then presented as a confusion matrix. This shows how many spectra have been correctly predicted to belong to its group. If correct predictions are low, the original LDA model is weak and needs improvement.

PCA and LDA can be combined by using the scores of the first few PCs as input for LDA. This is called PC-LDA and helps reduce the noise in the data used as input for LDA. LOOCV methodology remains the same for PC-LDA.

3. Results

3.1. FOS and JUN gene expression

Statistically significant difference for the FOS and JUN genes was detected in the comparison between the groups in all three analysis performed, analysis 1 (group 3 vs group 1), analysis 2 (group 4 vs group 1) and analysis 3 (group 5 vs group 1) (p less than 0.05) (Mann-Whitney test). FOS and JUN genes expression were decreased in the malign tumors together (group 3: PTC and FTC) (p = 0.0004 and p = 0.0004,

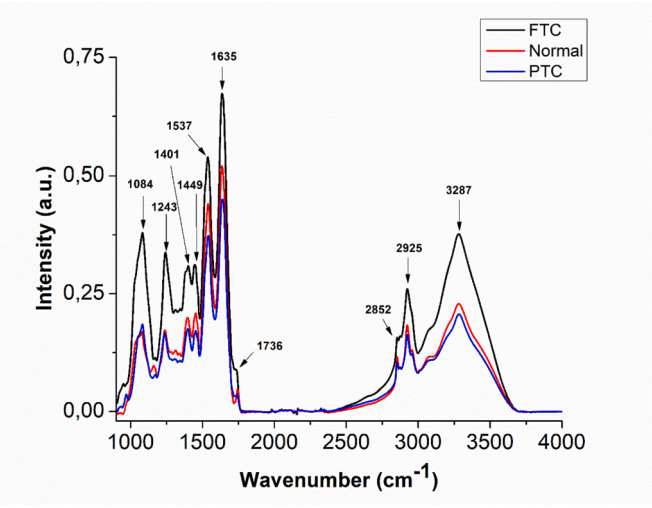

Fig. 3. Mean ATR-FTIR spectra of FTC, PTC and non-neoplastic tissues (Non-neoplastic).

Table 1
Characteristic bands in FTIR spectra and preliminary assigments of samples (NNT†, FTC‡ and PTC§).

Peak positions (cm^{-1})	Vibrations	Reference substancy
1084 cm^{-1}	$_{vs}PO_2^-$	Nucleic Acids/ Phospholipids
1243 cm^{-1}	$_{vs}PO_2^-$	Nucleic Acids
1401 cm^{-1}	$_{vs}CH_3$ and $_{vs}COO^-$	Proteins/Fatty Acids
1449 cm^{-1}	$_{vas}CH_3$	Proteins
1537 cm^{-1}	$_{v}C{=}O$ and $_{v}C{=}C$	Lipids
1635 cm^{-1}	β-sheet structure of amide I	Protein
1736 cm^{-1}	$_{v}C{=}O$	Lipids
2852 cm^{-1}	$_{vs}CH_2$	Lipids
2925 cm^{-1}	$_{vas}CH_2$	Lipids
3287 cm^{-1}	$_{vs}O{-}H$	Water/Protein

v: stretching vibration. vs: symetric stretching vibration. vas: asymetric stretching vibration.
†non-neoplastic thyroid.
‡ follicular thyroid carcinoma.
§ papillary thyroid carcinoma.

respectively) (Analysis 1); in the PTC samples (group 4) ($p = 0.0014$ and $p = 0.0014$, respectively) and in the FTC samples (group 5) ($p = 0.0033$ and 0.0032, respectively) in comparison with normal tissues (group 1) (Fig. 1). In PTC group, nine samples showed decreased expression (QR = 0.00 to 0.46 for FOS gene; QR = 0.11 to 0.42 for JUN gene) and one sample presented normal expression (QR = 0.51 for FOS gene; QR = 0.60 for JUN gene) in relation the normal samples. In FTC group, 100 % of the samples (seven) showed decreased expression for both genes (QR = 0.09 to 0.27 for FOS gene; QR = 0.07 to 0.21 for JUN gene) to that in NN tissues.

The potential diagnosis of FOS and JUN genes has been confirmed in the comparison between malignant tumors and benign tumors, with observation of statistically significant difference in all comparisons ($p \leq 0.05$). Both genes showed decreased expression in the malignant tumors together (group 3) ($p = 0.0032$ and 0.0025, respectively) (Analysis 4); in the PTC samples (group 4) ($p = 0.0375$ and $p = 0.0455$, respectively) (Analysis 5) and FTC samples (group 5) ($p = 0.0048$ and 0.0021, respectively) (Analysis 6) in comparison with BT samples (group 2). In the comparison between FTC and PTC (Analysis 7), statistically significant difference was observed only to the JUN gene, highlighting the decrease in expression in FTC when compared to PTC ($p = 0.0028$) (Fig. 2).

3.2. ATR-FTIR spectroscopy analysis

Ninety spectra were obtained in total (three spectra per sample). The number of spectra per group were 27 from PTC samples, 15 from FTC samples, 33 from BT samples (15 of adenomatous goiter, 12 of follicular adenoma and six of follicular hyperplasia samples) and 15 of NN samples.

Fig. 3 shows the mean spectrum of the evaluated groups. NN and PTC spectra are similar, and differ from FTC spectrum in intensities of bands related to nucleic acids (RNA and DNA) and phospholipids (1084 cm^{-1} and 1243 cm^{-1}), fatty acids and proteins (1401 cm^{-1}, 1449 cm^{-1}, 1635 cm^{-1} and 3287 cm^{-1}) and lipids (1537 cm^{-1}, 1736 cm^{-1}, 2852 cm^{-1} and 2925 cm^{-1}) (Fig. 3, Table 1).

PCA of NN, BT, PTC and FTC showed that FTC can be separated from NN, BT and PTC spectra. PCA of only spectra from BT samples showed that adenomatous goiter, follicular adenoma and follicular hyperplasia can be separated from each other. Loadings indicate differences in 840 (DNA), 967(DNA), 1103 (carbohydrates), 1155 (protein), 1231 (protein), and 1338 cm^{-1} (collagen) in partial separation of NN, BT, FTC, and PTC, while 1563 (nucleic acid), 1658 (protein), 1737 cm^{-1} (lipids) were responsible for separation of benign tumors (Fig. 4). PC-LDA LOOCV showed that NN, BT, FTC and PTC can be classified with 60, 70, 93 and 78 % efficiency, respectively (Table 2). Adenomatous goiter, follicular adenoma and follicular hyperplasia were classified with 93, 83, and 100 % efficiency, respectively by PC-LDA LOOCV (Table 3). These results suggest that NN tissue and benign tumors can be discriminated from thyroid carcinoma, as BT samples can also be distinguished from each other by ATR-FITR analysis.

4. Discussion

We show the potential of qRT-PCR and ATR-FTIR in diagnosis of thyroid cancer, the most common endocrine cancer. The present study found that FOS and JUN gene expression profiles were significantly lower in malignant tumor (PTC and FTC) samples compared to benign and healthy. ATR-FTIR spectroscopy of the samples followed by multivariate analysis could also identify folicular thyroid carcinoma with high efficiency, was significantly lower in the PTC and FTC samples when compared with normal tissues and benign lesions. This result favors the hypothesis that both genes present themselves as potential diagnostic molecular markers in thyroid cancer.

FOS and JUN genes are transcription factors associated with the development of different types of tumors. The FOS gene acts in several tumorigenic processes, which include cell motility, proliferation, tumor growth, metastasis and angiogenesis [41]. Krishna et al. [42] detected a decrease in C-FOS gene expression in patients with suspected oral squamous cell carcinoma (OSCC), associated with the potential responsible for the development of these tumors. The analysis was performed by comparing OSCC tumor tissues with normal oral mucosa tissues (control group), with reduced expression of the gene in the OSCC group compared to the control group, confirmed by complementary protein analysis. The JUN gene, first proto-oncogene described, encodes an AP-1 transcription factor, and also acting as an independent transcription factor [43]. Like FOS gene, this gene plays an important role in regulating cell proliferation and carcinogenic processes. Chen et al [44] identified that JUN is linked to extracellular signal translation processes in association with different transcription factors in PTC, not only linked to its FOS cofactor. Fry and Inoue [45] described that the protein encoded by JUN, transcription factor AP-1, is directly linked to the expression of an important checkpoint protein present in the G1/S phase of the cell cycle, regulating this process positively.

In this study, the expression profile of the FOS and JUN genes to be significantly lower in the PTC and FTC samples compared with NN tissues and benign lesions. Therefore, we hypothesize that decreased expression of the JUN gene in the malignant tumors could trigger a failure of proliferation control, as the AP-1 transcription complex may

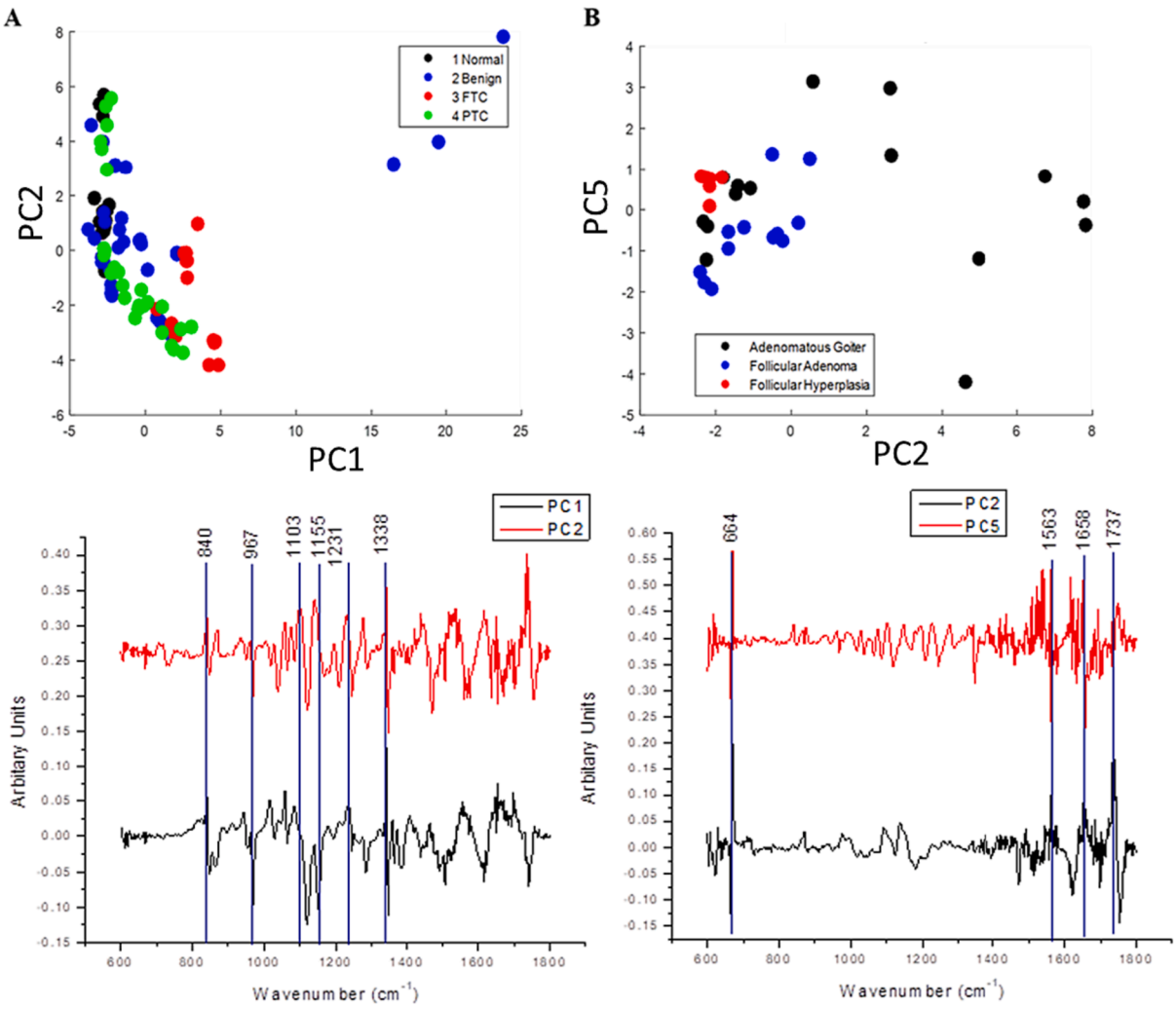

Fig. 4. PCA Analysis plots. A: Comparison between PTC, FTC, BT and NNT. B: Comparison between the benign tumors (Adenomatous goiter, Follicular adenoma and Follicular hyperplasia).

Table 2
The discriminant analysis of the main linear componente of NNT, BT, FTC and PTC.

	NNT	BT	FTC	PTC
NNT†	**9 (60 %)**	3 (20 %)	0	3 (20 %)
BT*	3 (9.1 %)	**23 (69.7 %)**	4 (12.1 %)	3 (9.1 %)
FTC‡	0	1 (6.7 %)	**14 (93.3 %)**	0
PTC§	1 (3.7 %)	3 (11.1 %)	2 (7.4 %)	**21 (77.8 %)**

† non-neoplastic thyroid.
* benign tumor.
‡ follicular thyroid carcinoma.
§ papillary thyroid carcinoma.

Table 3
The discriminant analysis of the main linear componente of Adenomatous Goiter, Follicular Adenoma and Follicular Hyperplasia.

	Adenomatous Goiter	Follicular Adenoma	Follicular Hyperplasia
Adenomatous Goiter	14 (93.3 %)	0	1 (6.7 %)
Follicular Adenoma	0	10 (83.3 %)	2 (16.7 %)
Follicular Hyperplasia	0	0	6 (100 %)

be correlated with genes responsible for processes such as apoptosis and cell repair, and the reduced expression of this gene can, consequently, favor different carcinogenic processes. Results of our study showed that FOS and JUN genes are promising molecular markers for the diagnosis of thyroid malignancies.

FTIR spectroscopy results suggest that thyroid cancer can be distinguished from normal, and that benign variants of thyroid cancer can also be distinguished.

The FTIR technique has advantages such as minimal sample preparation, in addition to being sensitive and specific in the non-invasive analysis of tissue composition [32]. The technique can be applied to variety of samples, including clinical Fine Needle Aspiration Biopsy (FNAB). Since the technique is non-destructive, the same sample can be reused after spectroscopy for molecular biology based diagnosis.

Studies in the literature have demonstrated the high capacity of FTIR spectroscopy to biologically characterize thyroid tumors though vibrational analysis and identification of bands in the infrared spectrum [37–38,46–49]. Depciuch et al [37] was able to specifically differentiate widely invasive follicular carcinoma (WI-FTC) from non-tumor tissues by observing changes in the absorbance bands for substances present in all cell structures, especially proteins and lipids. In their results, it is described that the most significant changes in the spectrum obtained between neoplastic and normal tissues was the region of the spectrum corresponding to functional groups from proteins, with lower absorbance intensity to NN tissues of thyroid. In another subsequent study,

Depciuch et al [38] was able to differentiate WI-FTC tumors from a benign tumor follicular adenoma. When compared, it was possible to observe that in the WI-FTC samples there were significant changes in the vibration of functional groups that comprise nucleic acids and proteins, corresponding to the present of PO_3^{-2} groups of DNA, RNA and phospholipids.

In addition to biochemical characterizing the lesions, studies such as Zancla et al. [46] was able to perform biochemical characterization even in specific calcified structures of PTC, called psammoma bodies, through the association of microscopy and FTIR spectroscopy called micro spectroscopy. They are associated with the detection of bands between 850 and 1100 cm^{-1}, which represent the detection of carboapatites, observed by PCA analysis of stretching in PO_4^{3-} group and modes of CO_3^{2-}. The spectral characterization and PCA analysis by FTIR spectroscopy have also been highlighted in the differentiation and classification of tissues with thyroid tumor manifestations [38,45,50]. Depciuch et al [38] was able to differentiate two thyroid tumor tissues of difficult histopathological differentiation (WI-FTC and follicular adenoma) with 65 % sensitivity and 75 % specificity, these percentages being of low impact for use in the diagnosis of this lesions.

In our study, we found PTC and FTC differ from normal and benign biochemically in terms of nucleic acid, phospholipids, fatty acids, lipids, and proteins. Multivariate analysis could classify FTC from NN, benign and PTC with 93 % efficiency, while PTC could be classified from other groups with 78 % efficiency. PTC showed considerable misclassification with benign (11 %). Benign lesion spectra could be classified from other groups with 70 % efficiency, showing misclassification with normal (9 %), PTC (9 %), and FTC (12 %). NN tissue spectra showed high misclassification with benign (20 %) and PTC (20 %), but no misclassification with FTC. This indicates that, based on results from this study, that ATR-FTIR can best identify FTC from other conditions. This is encouraging, since FTC has worse prognosis than PTC owing, among other factors, to difficulty in diagnosing the condition.

5. Conclusion

Gene expression studies suggest that FOS and JUN are underexpressed in malignant thyroid tumors when compared to normal tissues and benign tumors. This can be exploited to distinguish malignant from benign forms and normal tissues. ATR-FTIR could identify follicular thyroid carcinoma with high efficiency and also classify adenomatous goiter, follicular adenoma, and follicular hyperplasia (benign thyroid tumors) with 93, 83, and 100 % efficiency, respectively. Used in tandem, the two techniques, ATR-FTIR for mass screening and molecular biology for gene expression based confirmation, can be used to provide better diagnostic solutions for patients.

CRediT authorship contribution statement

João Paulo da Silva Queiroz: Methodology, Formal analysis, Writing – original draft. **Breno Pupin:** Methodology. **Tanmoy Tapobrata Bhattacharjee:** Formal analysis, Writing – review & editing. **Miyuki Uno:** Resources. **Roger Chammas:** Resources, Writing – review & editing. **Marco Aurélio Vamondes Kulcsar:** Resources, Writing – review & editing. **Renata de Azevedo Canevari:** Conceptualization, Methodology, Project administration, Resources, Funding acquisition, Writing – review & editing.

Declaration of Competing Interest

The authors declare the following financial interests/personal relationships which may be considered as potential competing interests: Renata de Azevedo Canevari reports financial support was provided by State of Sao Paulo Research Foundation.

Data availability

Data will be made available on request.

Acknowledgments

This research was supported by Fundação de Amparo a Pesquisa do Estado de São Paulo - FAPESP (Project n° 2009/18440-1, no 2013/14464-9 and no 2019/10211-5).

Ethics Approval and Consent to Participate

This study was approved by the Research Ethics Committee of the University of Vale do Paraíba (3,620,075/CEP/2019);

References

[1] S. Vaccarella, S. Franceschi, F. Bray, C.P. Wild, M. Plummer, L.D. Maso, Worldwide Thyroide-Cancer Epidemic? The Increasing Impact of Overdiagnosis, N. Engl. J. Med. 375 (7) (2016) 614–617.
[2] S. Vaccarella, L. Dal Maso, M. Laversanne, F. Bray, M. Plummer, S. Franceschi, The impact of diagnostic changes on the rise in thyroid cancer incidence: A population-based study in selected high-resource countries, Thyroid 25 (10) (2015) 1127–1136.
[3] L. Davies, L.G.T. Morris, M. Haymart, A.Y. Chen, D. Goldenberg, J. Morris, et al., American Association of Clinical Endocrinologists and American College of Endocrinology Disease State Clinical Review: the Increasing Incidence of Thyroid Cancer, Endocr. Pract. 21 (6) (2015) 686–696.
[4] H. Sung, J. Ferlay, R.L. Siegel, M. Laversanne, I. Soerjomataram, A. Jemal, et al., Global Cancer Statistics 2020: GLOBOCAN Estimates of Incidence and Mortality Worldwide for 36 Cancers in 185 Countries, CA Cancer J. Clin. (2021) 1–41.
[5] INCA. Estimativa 2020. Incidência de Câncer no Brasil. 2020. 7–117 p.
[6] S. Kure, R. Wada, Z. Naito, Relationship between genetic alterations and clinicopathological characteristics of papillary thyroid carcinoma, Med. Mol. Morphol. [Internet]. (2019) 1–6, https://doi.org/10.1007/s00795-019-00217-6. Available from:.
[7] E.O. Gur, S. Karaisli, S. Haciyanli, E. Kamer, H. Genc, K. Atahan, et al., Multifocality related factors in papillary thyroid carcinoma, Asian J. Surg. [Internet]. 42 (1) (2018) 297–302, https://doi.org/10.1016/j.asjsur.2018.05.004. Available from:.
[8] S.H. Jeong, H.S. Hong, E.H. Lee, Can nodular hyperplasia of the thyroid gland be differentiated from follicular adenoma and follicular carcinoma by ultrasonography? Ultrasound Q. 32 (4) (2016) 349–355.
[9] N.A. Cipriani, S. Nagar, S.P. Kaplan, M.G. White, T. Antic, P.M. Sadow, et al., Follicular Thyroid Carcinoma : How Have Histologic Diagnoses Changed in the Last Half-Century and What Are the Prognostic Implications ? Thyroid Cancer Nodules. 25 (11) (2015) 1209–1216.
[10] L.J. Der, Thyroid Cancer in Thyroid Nodules Diagnosed Using Ultrasonography and Fine Needle Aspiration Cytology, J. Med. Ultrasound [Internet]. 18 (3) (2010) 91–104, https://doi.org/10.1016/S0929-6441(10)60014-8. Available from:.
[11] P. Dalquen, B. Rashed, A. Hinsch, R. Issa, T. Clauditz, A. Luebke, et al., Fine-needle aspiration (FNA) of the thyroid gland : Analysis of discrepancies between cytological and histological diagnoses, Pathologe 37 (5) (2016) 465–472.
[12] S.H. Ahn, S.Y. Park, C.S. Il, Comparison of Consecutive Results from Fine Needle Aspiration and Core Needle Biopsy in Thyroid Nodules, Endocr. Pathol. 28 (4) (2017) 332–338.
[13] D. Zhang, X. Liu, B. Wei, G. Qiao, T. Jiang, Z. Chen, Plasma lncRNA GAS8-AS1 as a Potential Biomarker of Papillary Thyroid Carcinoma in Chinese Patients, Int J. Endocrinol. (2017) 1–6.
[14] Y.Y. Jung, J.H. Yoo, E.S. Park, M.K. Kim, T.J. Lee, B.Y. Cho, et al., Clinicopathologic correlations of the BRAF V600E mutation, BRAF V600E immunohistochemistry, and BRAF RNA in situ hybridization in papillary thyroid carcinoma, Pathol. – Res. Pract. [Internet]. 211 (2) (2015) 162–170, https://doi.org/10.1016/j.prp.2014.10.005. Available from:.
[15] J.M. Pita, A. Banito, B.M. Cavaco, V. Leite, Gene expression profiling associated with the progression to poorly differentiated thyroid carcinomas, Br. J. Cancer [Internet]. 101 (10) (2009) 1782–1791, https://doi.org/10.1038/sj.bjc.6605340. Available from:.
[16] Y. Wang, J. Gao, X. Meng, Z. Wang, DNA microarray-based resonance light scattering assay for multiplexed detection of DNA mutation in papillary thyroid cancer, R. Soc. Chem. (2018).
[17] J. Hu, C. Li, C. Liu, S. Zhao, Y. Wang, Z. Fu, Expressions of miRNAs in papillary thyroid carcinoma and their associations with the clinical characteristics of PTC, Cancer Biomark. 18 (1) (2017) 87–94.
[18] F. Nabhan, M.D. Ringel, Thyroid Nodules and Cancer Management Guidelines: Comparisons and Controversies, Endocr. Relat. Cancer 24 (2) (2017) 1–24.
[19] G.C. Penna, F. Vaisman, M. Vaisman, M. Sobrinho-Simões, P. Soares, Molecular Markers Involved in Tumorigenesis of Thyroid Carcinoma: Focus on Aggressive Histotypes, Cytogenet. Genome Res. (2017) 194–207.

[20] V. Marotta, C. Sciammarella, A. Colao, A. Faggiano, Application of molecular biology of differentiated thyroid cancer for clinical prognostication, Endocr. Relat. Cancer 23 (11) (2016) 499–515.
[21] S.J. Hsiao, Y.E. Nikiforov, Molecular approaches to thyroid cancer diagnosis, Endocr. Relat. Cancer 21 (5) (2014) 301–313.
[22] S. Zolotov, Genetic Testing in Differentiated Thyroid Carcinoma : Indications and Clinical Implications, Rambam Maimonides Med. J. 7 (1) (2016) 110.
[23] C. Xiao, Y. Huang, Q. Gao, Z. Feng, Q. Li, Z. Liu, Expression of activator protein-1 in papillary thyroid carcinoma and its clinical significance, World J. Surg. Oncol. 17 (25) (2019) 1–5.
[24] H. Dralle, A. Machens, J. Basa, V. Fatourechi, S. Franceschi, I.D. Hay, et al., Follicular cell-derived thyroid cancer, Nat. Rev. [Internet]. 1 (15077) (2015) 1–19, https://doi.org/10.1038/nrdp.2015.77. Available from:.
[25] M. Xing, Molecular pathogenesis and mechanisms of thyroid cancer. Nat Rev [Internet]. 2013;13:184–99. Available from: https://doi.org/10.1038/nrc3431.
[26] Z. Li, X. Xu, M. Luo, J. Hao, S. Zhao, W. Yu, et al., Activator Protein-2β Promotes Tumor Growth and Predicts Poor Prognosis in Breast Cancer, Cell. Physiol. Biochem. 47 (2018) 1925–1935.
[27] M. Burotto, V.L. Chiou, J.-M. Lee, E.C. Kohn, The MAPK pathway across different malignancies: A new perspective, Cancer 120 (22) (2014) 3446–3456.
[28] C. Buffet, K. Hecale-Perlemoine, L. Bricaire, F. Dumont, C. Baudry, F. Tissier, et al., DUSP5 and DUSP6, two ERK specific phosphatases, are markers of a higher MAPK signaling activation in BRAF mutated thyroid cancers, PLoS One 12 (9) (2017) 1–24.
[29] C. Kendall, M. Isabelle, F. Bazant-Hegemark, J. Hutchings, L. Orr, J. Babrah, et al., Vibrational spectroscopy: A clinical tool for cancer diagnostics, Analyst 134 (6) (2009) 1029–1045.
[30] F.M. Lyng, I.R.M. Ramos, O. Ibrahim, H.J. Byrne, Vibrational microspectroscopy for cancer screening, Appl. Sci. 5 (1) (2015) 23–35.
[31] O.J. Old, L.M. Fullwood, R. Scott, G.R. Lloyd, L.M. Almond, N.A. Shepherd, et al., Vibrational spectroscopy for cancer diagnostics, Anal. Methods 6 (12) (2014) 3901–3917.
[32] G. Bellisola, C. Sorio, Infrared spectroscopy and microscopy in cancer research and diagnosis, Am. J. Cancer Res. 2 (1) (2012) 1–21.
[33] M. Kyriakidou, J. Anastassopoulou, A. Tsakiris, M. Koui, T. Theophanides, FT-IR spectroscopy study in early diagnosis of skin cancer, In Vivo (Brooklyn). 31 (6) (2017) 1131–1137.
[34] Z. Movasaghi, S. Rehman, I. Rehman, Fourier Transform Infrared (FTIR) Spectroscopy of Biological Tissues, Appl. Spectrosc. Rev. 43 (2008) 134–179.
[35] A.A. Bunaciu, V.D. Hoang, H.Y. Aboul-Enein, Applications of FTIR Spectrophotometry in Cancer Diagnostics, Crit. Rev. Anal. Chem. 45 (2015) 156–165.
[36] A.A. Bunaciu, S. Fleschin, H.Y. Aboul-Enein, Cancer diagnosis by FT-IR Spectrophotometry, Rev. Roum. Chim. 60 (5–6) (2015) 415–426.
[37] J. Depciuch, A. Stanek-Widera, D. Lange, M. Biskup-Frużyńska, J. Stanek-Tarkowska, W. Czarny, et al., Spectroscopic analysis of normal and neoplastic (WI-FTC) thyroid tissue, Spectrochim. Acta - Part A Mol. Biomol. Spectrosc. 204 (2018) 18–24.
[38] J. Depciuch, A. Stanek-Widera, D. Skrzypiec, D. Lange, M. Biskup-Frużyńska, K. Kiper, et al., Spectroscopic identification of benign (follicular adenoma) and cancerous lesions (follicular thyroid carcinoma) in thyroid tissues, J. Pharm. Biomed. Anal. 170 (2019) 321–326.
[39] R.M. da Silva, M.J. Chagas, O.AB. De, B. Pupin, R.D.A. Canevari, Poder diagnóstico de genes da via MAPK/ERK em lesões de tireoide. XXII Encontro Lat Am Iniciação Científica, XVIII Encontro Lat Am Pós-Graduação e VIII Encontro Iniciação à Docência - Univ do Val do Paraíba, São José dos Campos. (2018) 1–6.
[40] K.J. Livak, T.D. Schmittgen, Analysis of relative gene expression data using real-time quantitative PCR and the 2(-Delta Delta C(T)) Method, Methods 25 (4) (2001) 402–408.
[41] P. Pallante, R. Sepe, A. Federico, F. Forzati, M. Bianco, A. Fusco, CBX7 Modulates the Expression of Genes Critical for Cancer Progression, PLoS One 9 (5) (2014) 1–12.
[42] A. Krishna, M.L.B. Bhatt, B. Bhatt, V. Singh, S. Singh, P.K. Gangwar, et al., Differential Expression of c-FOS Proto-Oncogene in Normal Oral Mucosa versus Squamous Cell Carcinoma, Asian Pacific J. Cancer Prev. 19 (2018) 867–874.
[43] Z. Liu, G. Jiang, J. Tang, H. Wang, G. Feng, F. Chen, et al., c-Fos over-expression promotes radioresistance and predicts poor prognosis in malignant glioma, Oncotarget 7 (40) (2016) 65946–65956.
[44] W. Chen, Q. Liu, Y. Lv, D. Xu, W. Chen, J. Yu, Special role of JUN in papillary thyroid carcinoma based on bioinformatics analysis, World J. Surg. Oncol. 15 (119) (2017) 1–7.
[45] E.A. Fry, K. Inoue, Aberrant expression of ETS1 and ETS2 proteins in cancer, Cancer Rep. Rev. 2 (3) (2018) 1–23.
[46] A. Zancla, S. De Santis, G. Sotgiu, C. Taffon, A. Crescenzi, M. Orsini, Micro-FTIR spectroscopy as robust tool for psammoma bodies detection in papillary thyroid carcinoma, Spectrochim. Acta - Part A Mol. Biomol. Spectrosc. [Internet]. 2020; 229:1–6. Available from: 18 https://doi.org/10.1016/j.saa.2019.117984.
[47] M. Wu, W. Zhang, P. Tian, X. Ling, Z. Xu, Intraoperative diagnosis of thyroid diseases by fourier transform infrared spectroscopy based on support vector machine, Int. J. Clin. Exp. Med. 9 (2) (2016) 2351–2358.
[48] X. Zhang, Y. Xu, Y. Zhang, L. Wang, C. Hou, X. Zhou, et al. Intraoperative Detection of Thyroid Carcinoma by Fourier Transform Infrared Spectrometry, J. Surg. Res. [Internet]. 2011;171:650–6. Available from: https://doi.org/10.1016/j.jss.2010.05.031.
[49] Y. Liu, Y. Xu, Y. Liu, Y. Zhang, D. Wang, D. Xiu, et al., Detection of cervical metastatic lymph nodes in papillary thyroid carcinoma by Fourier transform infrared spectroscopy, Br. J. Surg. 98 (3) (2011) 380–384.
[50] D. Martinez-Marin, H. Sreedhara, V.K. Varmab, C. Eloyc, M. Sobrinho-Simões, A. Kajdacsy-Ballaa, et al., Accounting for tissue heterogeneity in infrared spectroscopic imaging for accurate diagnosis of thyroid carcinoma subtypes, Vib. Spectrosc 91 (2018) 77–82.